



Contraction-Expansion and the Effects on the Aquiferous System in the Demosponge *Halichondria panicea*

Josephine Goldstein^{1,2*}, Nicklas Bisbo², Peter Funch² and Hans Ulrik Riisgård¹

¹ Marine Biological Research Centre, Department of Biology, University of Southern Denmark, Kerteminde, Denmark,

² Department of Biology – Genetics, Ecology and Evolution, Aarhus University, Aarhus, Denmark

OPEN ACCESS

Edited by:

Youji Wang,
Shanghai Ocean University, China

Reviewed by:

Russell Wyeth,
St. Francis Xavier University, Canada
Tibor Kiss,
Hungarian Academy of Sciences,
Hungary

*Correspondence:

Josephine Goldstein
jgoldstein@biology.sdu.dk

Specialty section:

This article was submitted to
Aquatic Physiology,
a section of the journal
Frontiers in Marine Science

Received: 13 May 2019

Accepted: 11 February 2020

Published: 26 February 2020

Citation:

Goldstein J, Bisbo N, Funch P
and Riisgård HU (2020)
Contraction-Expansion
and the Effects on the Aquiferous
System in the Demosponge
Halichondria panicea.
Front. Mar. Sci. 7:113.
doi: 10.3389/fmars.2020.00113

Contractile behavior is common among sponges despite their lack of nerves and muscles. As sessile filter-feeders, sponges rely on water with suspended food particles being pumped through their aquiferous system. During contractions, however, the water flow is being reduced and eventually shut down. Yet, purpose and underlying pathways of contractile behavior have remained largely unclear. Here, we document the external and internal morphology of contracted and expanded single-ostium explants of the demosponge *Halichondria panicea*. We show that contraction-expansion dynamics can occur spontaneously (in untreated explants) and can be induced by exposure to chemical messengers such as γ -aminobutyric acid (GABA, 1 mM) and L-glutamate (L-Glu, 1 mM), or to inedible ink particles (4 mg L⁻¹). The neurotransmitter GABA triggered similar contraction-expansion dynamics in *H. panicea* as observed in untreated explants. The effects of GABA-induced contraction-expansion events on the aquiferous system were investigated using scanning electron microscopy (SEM) on cryofractured explants. Our findings suggest that contraction-expansion affects the entire aquiferous system of *H. panicea*, including ostium, ostia, in- and excurrent canals and apopyles.

Keywords: contraction, aquiferous system, functional morphology, SEM, chemical messengers, inedible particles, marine demosponge

INTRODUCTION

Sponges are sessile filter-feeders that pump water by means of choanocytes (Reiswig, 1975; Asadzadeh et al., 2019) which are specialized flagellated cells that efficiently retain particles down to $\sim 0.1 \mu\text{m}$ on their microvilli collars (Riisgård and Larsen, 2000). Ambient water is drawn through numerous inhalant openings (ostia) into an incurrent canal system, where it enters many choanocyte chambers (CCs) through prosopyles, passes microvillar collar-sieves, exits the CC through apopyles and leaves the sponge via an excurrent canal system that finally leads to an exhalant opening, the osculum (Larsen and Riisgård, 1994). Contractions can effectively restrict or stop the water flow through a sponge (Reiswig, 1971; Riisgård et al., 2016; Kumala et al., 2017; Ludeman et al., 2017; Goldstein et al., 2019) and have been suggested to protect the filter-pump, for instance during periods with high loads of re-suspended sediment (Elliott and Leys, 2010; Bannister et al., 2012; Leys, 2015; Grant et al., 2019).

Sponges lack conventional nerves and muscles but contract in response to environmental stimuli (Parker, 1910; McNair, 1923; Reiswig, 1971; Elliott and Leys, 2007, 2010; Tompkins-MacDonald and Leys, 2008; Leys, 2015), or following endogenously controlled contraction-expansion cycles (Reiswig, 1971; Nickel, 2004). Signaling in demosponges is poorly understood but probably involves non-motile primary sensory cilia (Nickel, 2010; Ludeman et al., 2014; Leys, 2015), conduction pathways based on chemical messengers (Ellwanger and Nickel, 2006; Ellwanger et al., 2007) and an antagonistic contractile apparatus, most likely mediated by the pinacoderm as effector and the water pressure generated by the choanocytes (Nickel et al., 2011). Interaction of this “neural toolkit” (Leys, 2015) results in slow peristaltic-like waves of contraction traveling through the aquiferous system of a sponge (Elliott and Leys, 2007; Goldstein et al., 2019). An improved understanding of the functional morphology underlying contraction-expansion events in sponges may provide important insights into the control of water flow through the aquiferous system.

Halichondria panicea is a common marine demosponge widely distributed in temperate coastal regions of the northern hemisphere (Erpenbeck et al., 2004). Its contractile behavior regarding osculum closure (Riisgård et al., 2016; Kumala et al., 2017) and associated constriction of the excurrent canals (Goldstein et al., 2019) has been described, but the role of other aquiferous elements is unclear. Here, we determine the trigger potential of neurotransmitters and inedible particles compared to spontaneous (untreated conditions) contraction-expansion events in single-osculum explants of *H. panicea*. Subsequently we use these findings to induce similar contraction-expansion events as observed in untreated explants and study the resulting effects on the aquiferous system in explants fixed in different contraction-expansion phases using scanning electron microscopy (SEM).

MATERIALS AND METHODS

Cultivation of Sponge Explants

Sponge explants were obtained from *Halichondria panicea* specimens collected in the inlet of Kerteminde Fjord, Denmark (55°26'59"N, 10°39'40"E). Small pieces (5–10 mm³) were cut from the exhalant chimneys of collected sponges and individually placed on glass slides in flow-through aquaria with aerated bio-filtered seawater (15–25 psu, 15°C). After attachment to glass slides and development of an osculum, the single-osculum explants (i.e. functional aquiferous modules; Kealy et al., 2019), were fed with *Rhodomonas salina* algae and bacteria growing in the algal culture (cf. Kumala et al., 2017).

Video-Microscope Observation of Contraction-Expansion Dynamics

The contractile responses of explants exposed to either γ -aminobutyric acid (GABA), L-glutamic acid (L-Glu), or to inedible particles (calligraphy ink) were compared to spontaneous contractions of untreated explants (i.e. seawater

control). Contractile behavior of single-osculum explants was observed in 1 L aquaria with bio-filtered seawater (20 psu, 15°C) under constant mixing with a magnetic stirrer. Only actively pumping explants, with fully expanded osculum at the start of experiments, were included. Contraction-expansion dynamics of explants under different treatments were documented in long-term (12–24 h) time-lapse image sequences of the osculum cross-sectional area (OSA , mm²) and the side-view projected area (A , mm²) of single-osculum explants using a video-microscope (Leica MZ8) with a USB 3.0 industrial camera (Imaging-source, DFK23UM021) and image acquisition software (IC Capture 2.3). We analyzed temporal changes in OSA and A with imaging software (ImageJ, 1.50f) to identify distinct contraction-expansion events. These events were defined by reduction in the initial (i.e. before contraction) maximum osculum cross-sectional area (OSA_{max}) and projected area (A_{max}), osculum closure ($OSA = 0$ mm²) and corresponding minimum projected area (A_{min}), respectively, and subsequent expansion to a second maximum (i.e. after contraction). Spontaneous contraction-expansion events which occurred randomly within 24 h in untreated explants were selected from the time-lapse sequences. Trigger concentrations of GABA, L-Glu and ink which reliably induced contraction-expansion within <1 h were determined from dose-response experiments. We additionally tested the antagonistic effect of different concentrations of L-menthol (crystals dissolved in seawater) during GABA-induced contraction-expansion cycles (positive control). The intensity and duration of induced versus spontaneous contraction-expansion cycles was determined in replicate explants ($n = 6$ per treatment). For comparison across treatments, time (t , min) was standardized by setting $t_0 = 0$ as the mean time of osculum closure or as the mean time of minimum relative projected area defined by the confidence interval [$(A_{min} - 0.025)$, $(A_{min} + 0.025)$]. The relative osculum cross-sectional area and relative projected area were calculated as:

$$OSA_r = OSA/OA_{max}, \quad (1)$$

$$A_r = A/A_{max}. \quad (2)$$

where OSA_{max} and A_{max} correspond to $OSA_r = 1$ and $A_r = 1$, respectively. The duration of each contraction-expansion cycle was estimated as the total duration of the phase of contraction (I), the contracted phase (II), the phase of expansion (III), and the subsequent expanded phase until the onset of a new contraction (IV; **Figure 1**). Speeds of contraction (v_I , $\Delta OSA_r \text{ min}^{-1}$ and $\Delta A_r \text{ min}^{-1}$) and expansion (v_{III} , $\Delta OSA_r \text{ min}^{-1}$ and $\Delta A_r \text{ min}^{-1}$) were calculated for each explant from the slopes of linear regression lines for OSA_r and A_r during phase I and III, respectively. From relative changes in A during contraction ($\Delta A_I, \%$) and during expansion ($\Delta A_{III}, \%$) and the height (h , mm) of explants, the corresponding changes in explant volume during contraction ($\Delta V_I, \%$) and expansion ($\Delta V_{III}, \%$) were estimated using the volume (V , mm³) equation for axisymmetric conical explants (Goldstein et al., 2019):

$$V = \pi A^2/3h. \quad (3)$$

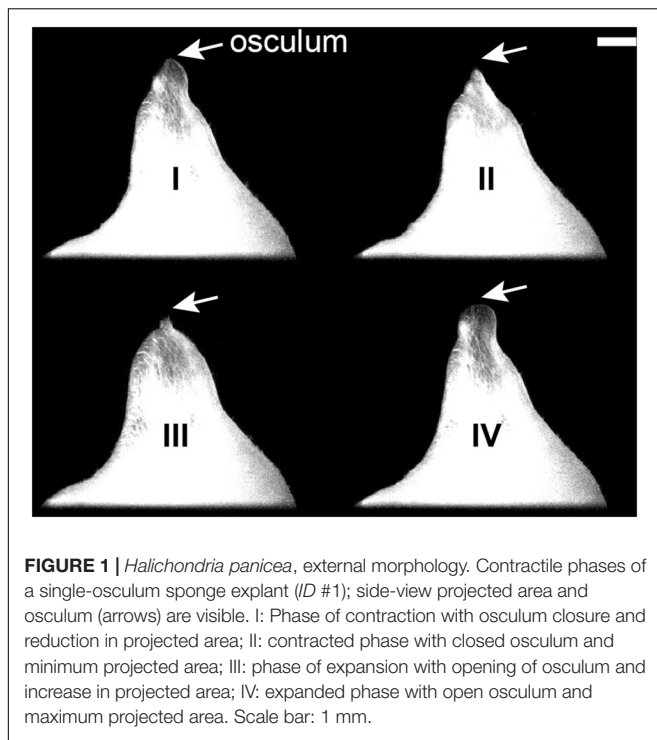


FIGURE 1 | *Halichondria panicea*, external morphology. Contractile phases of a single-ostium sponge explant (*ID* #1); side-view projected area and osculum (arrows) are visible. I: Phase of contraction with osculum closure and reduction in projected area; II: contracted phase with closed osculum and minimum projected area; III: phase of expansion with opening of osculum and increase in projected area; IV: expanded phase with open osculum and maximum projected area. Scale bar: 1 mm.

Scanning Electron Microscopy

Single-ostium explants ($n = 4$) with expanded oscula were transferred to small containers with 30 mL sterile filtered ($0.2 \mu\text{m}$) seawater from the cultivation tank. These explants were exposed to 1 mM GABA for various exposure times (t_{GABA} , min). Exposure times to GABA were estimated based on the osculum-opening degree of explants to induce different phases of contraction-expansion, including I: contracting, $t_{\text{GABA}} = 41$ min; II: contracted, $t_{\text{GABA}} = 48$ min; III: expanding, $t_{\text{GABA}} = 54$ min and IV: expanded phase, $t_{\text{GABA}} = 0$ min (**Figure 1**). The external morphology of explants in these contractile phases was documented stereo-microscopically prior to and after fixation for scanning electron microscopy (SEM). Explants were fixed for SEM by addition of 2% OsO_4 in 0.1 M cacodylate buffer (6 mL) and left overnight in the fixative at 4°C . Afterward they were transferred to containers with sterile filtered seawater from the cultivation tank and rinsed for 15 min; this step was repeated three times. After a final rinsing for 72 h in sterile filtered seawater, explants were dehydrated in a graded ethanol series, placed in a Parafilm sleeve with 100% ethanol and submerged in liquid nitrogen until the ethanol had solidified. The explants were then cryofractured with a razor blade, transferred to 100% ethanol at room temperature, critical point dried (EMS860) and sputter coated with a 45 nm thick gold layer (Edwards S150B). Cryofractured specimens were examined using a FEI NOVA NanoSEM 600 scanning electron microscope operated at 5 kV using an ETD detector. Diameter (D , μm) of osculum, ostia, canals and apophyses were measured using imaging software NIS-Elements D 4.10.04 (Nikon Instruments) and ImageJ, 1.50f. The degree of shrinkage due to fixation was estimated from measurements of the osculum diameter.

Statistical Analyses

Statistical data analyses were performed in R version 3.1.3 (R Core Team, 2015) using R package “lme4” (Bates et al., 2014). Generalized linear models (GLMs) were parameterized with Gamma error structure (meeting the assumptions of normal distribution, homoscedasticity and independence of residuals) to test for differences between the rates of contraction (v_{I}) and expansion (v_{III}) of the osculum cross-sectional area (OSA) or projected area (A) of untreated explants. Generalized linear mixed-effect models (GLMMs) with Gamma error structure were fitted to investigate variability in OSA or A across treatments (untreated, GABA, L-Glu and inedible particles; fixed effect) when correcting for individual variation (*ID*#; random effect). *Post hoc* analysis was conducted by multiple comparisons of means using Tukey contrasts (significance level $p < 0.05$) from R package “multcomp” (Hothorn et al., 2013). While OSA was similar across the experimental conditions (GLMM, $t = 1.6$, $p > 0.366$), A varied significantly among the explants exposed to different treatments (GLMM, $t = 10.3$, $p < 0.029$; Tukey *post hoc* test, group 1: GABA, group 2: spontaneous and L-Glu, group 3: ink particles). Using GLMMs with Gamma error structure, we then compared the rates of contraction/expansion, duration of the contracted phase in OSA or A , and the volume change during contraction/expansion, respectively, after exposure to different treatments (GABA, L-Glu or inedible particles; fixed effect) to spontaneous (untreated) contraction-expansion dynamics by taking into account variable A (fixed effect) and individual variation of explants (*ID*#; random effect). Similar GLMMs were parameterized to investigate changes in the diameter (D) of ostia, canals and apophyses during different contractile phases of explants (fixed effect) by correcting for individual variation (*ID*#; random effect).

RESULTS

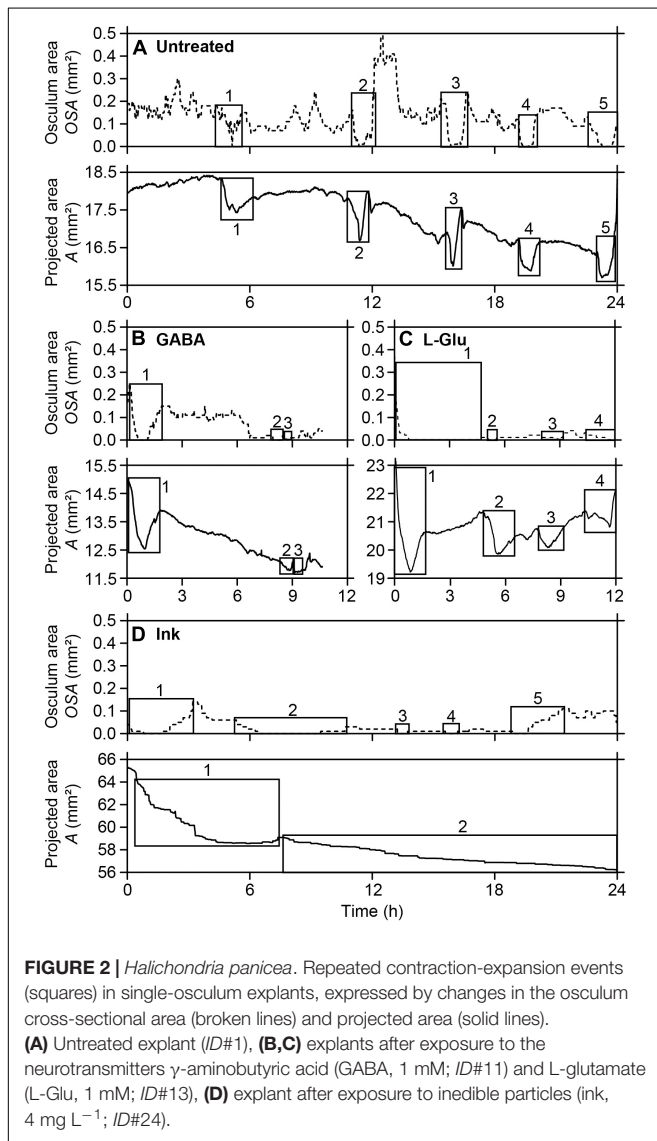
Spontaneous and Induced Contractions

Spontaneous contraction-expansion events in *Halichondria panicea* explants under untreated conditions showed a cyclic pattern (**Figure 2A**). Five spontaneous contraction-expansion events, including contraction phase (I), contracted phase (II), and expansion phase (III) were observed in a mean (\pm SD) interval of 4.4 ± 1.3 h (i.e. subsequent expanded phase, IV) within 24 h (**Figure 2A**). Spontaneous contraction-expansion events initiated randomly after >1 h in untreated sponge explants (*ID*#1–6; **Table 1**). Selected events included oscular contraction by -100% within 43 ± 21 min, complete osculum closure ($\text{OSA} = 0$) for 24 ± 12 min and subsequent osculum expansion by $130 \pm 88\%$ within 74 ± 39 min (**Table 2**). Corresponding contraction and expansion speeds were $-0.025 \pm 0.010 \Delta\text{OSA}_r \text{ min}^{-1}$ and $0.022 \pm 0.020 \Delta\text{OSA}_r \text{ min}^{-1}$, respectively (**Table 2**). The total duration of a spontaneous contraction-expansion cycle was 6.7 h (phases I + II + III + IV = $0.7 + 0.4 + 1.2 + 4.4$ h). Changes in the projected area of the explants occurred 18 ± 39 min after osculum closure (**Figure 3A**) and were characterized by a contraction rate $-0.001 \pm 0.001 \Delta A_r \text{ min}^{-1}$, a contracted phase 7 ± 2 min and a subsequent expansion rate $-0.002 \pm 0.002 \Delta A_r \text{ min}^{-1}$. Changes in A due to contraction and expansion

TABLE 1 | *Halichondria panicea*. Dimensions of (expanded) sponge explants before exposure to different treatments.

Treatment	ID#	OSA _{max} (mm ²)	A _{max} (mm ²)	H (mm)	V _{max} (mm ³)
Untreated	1–6	0.30 ± 0.14	19.1 ± 8.0	4.3 ± 1.3	96.1 ± 60.9
GABA (1 mM)	7–12	0.16 ± 0.09	9.5 ± 3.9	2.6 ± 0.6	38.4 ± 24.7
L-Glu (1 mM)	13–18	0.18 ± 0.14	14.8 ± 6.8	3.5 ± 1.4	74.8 ± 65.4
Ink particles (4 mg L ⁻¹)	19–24	0.24 ± 0.11	46.9 ± 18.8	5.6 ± 1.2	438.8 ± 236.0

OSA_{max} (= OSA for OSA_r = 1, Eq. 1): maximum (initial) osculum cross-sectional area, A_{max} (= A for A_r = 1, Eq. 2): maximum (initial) projected area, h: explant height, V_{max}: maximum (initial) explant volume (Eq. 3). Means ± SD are shown.



($-4.9 \pm 3.0\%$ and $5.2 \pm 1.8\%$, respectively), were reflected by changes in explant volume by $-9.6 \pm 5.7\%$ and $9.5 \pm 3.0\%$ (Table 3). Untreated *H. panicea* explants showed comparable contraction and expansion speeds of OSA (GLM, $t_{5,1,10} = 0.38$, $p = 0.712$) and A (GLM, $t_{6,5,10} = -1.77$, $p = 0.108$).

Exposure of explants to either GABA (1 mM), L-Glu (1 mM), or inedible ink (4 mg L⁻¹; particle density $\sim 10^5$ mL⁻¹, diameter

$3.3 \pm 1.0 \mu\text{m}$) reliably induced contractile responses of variable dynamics within 15–30 min (Supplementary Figures S1A–C). Repeated contraction-expansion cycles with mean expanded phases of 3.6 ± 4.6 , 1.9 ± 0.7 , and 3.8 ± 1.0 h, respectively, were observed after exposure of explants to GABA, L-Glu or ink. Continuous exposure to GABA, L-Glu and ink for >1 h resulted in incomplete recovery of OSA and A (Figures 2B–D). The GABA-induced contraction-expansion cycle of explants (ID#7–12, Table 1) was characterized by comparable total duration (5.4 h; Figure 2B), rate of contraction/expansion ($-0.032 \pm 0.023 \Delta\text{OSA}_r \text{ min}^{-1}$ and $0.015 \pm 0.008 \Delta\text{OSA}_r \text{ min}^{-1}$, respectively), and duration of contracted phase (22 ± 9 min) as observed in untreated explants (Tables 2–4). Similar as during spontaneous contractions, changes in A followed osculum closure by 15 ± 28 min (Figure 3B). Contractile responses to GABA further included similar changes in explant volume by $-15.3 \pm 10.3\%$ and $11.1 \pm 12.3\%$ as during spontaneous contractions (Tables 3, 4). In contrast to untreated conditions, exposure of explants (ID #13–18; Table 1) to L-Glu triggered significantly faster contraction of A ($-0.004 \pm 0.003 \Delta A_r \text{ min}^{-1}$), a prolonged contracted phase of both the OSA (84 ± 85 min) and A (12 ± 6 min), and significantly slower expansion of A ($-0.4 \pm 0.2 \times 10^{-3} \Delta A_r \text{ min}^{-1}$; (Figure 3C and Tables 2–4). These changes in A after exposure to L-Glu were also expressed by an observed maximum volume change $-21.6 \pm 7.2\%$ during contraction (Tables 3, 4). The L-Glu-induced contraction-expansion cycle was shortened to 4.7 h (Figure 2C and Table 2). Ink-triggered contractions (ID#19–24; Table 1) were characterized by comparable oscular contraction/expansion speeds ($-0.019 \pm 0.018 \Delta\text{OSA}_r \text{ min}^{-1}/0.028 \pm 0.008 \Delta\text{OSA}_r \text{ min}^{-1}$), duration of osculum closure (38 ± 20 min), total contraction-expansion cycle (5.7 h; Figure 2D and Table 2) and volume changes ($-13.9 \pm 7.5\%$ and $5.5 \pm 4.9\%$; Table 3) as observed during spontaneous contractions, while the contracted phase of A was significantly extended (42 ± 64 min; Figure 3D and Tables 3, 4). Contraction-expansion events resembling spontaneous behavior were induced by short-term (≤ 1 h) exposure of explants to GABA (1 mM). The contraction-inducing effect of GABA was inhibited by addition of L-menthol ($1-100 \text{ mg L}^{-1}$; Supplementary Figure S2).

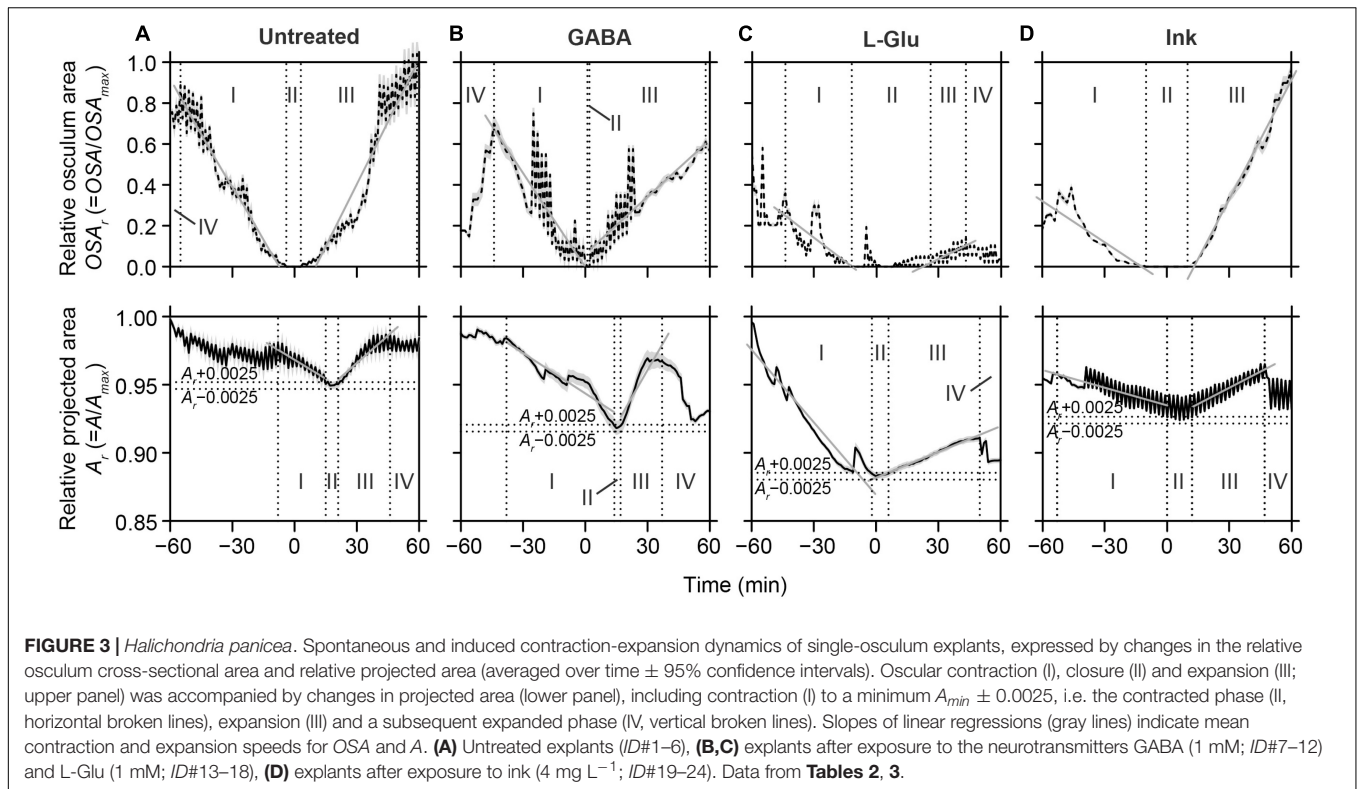
Contraction-Expansion of the Aquiferous System

External and internal morphology of single-osculum explants were investigated using SEM (Figure 4). Before fixation,

TABLE 2 | *Halichondria panicea*. Spontaneous (i.e. untreated conditions) and induced (by exposure to the neurotransmitters GABA, L-Glu or ink particles) contraction-expansion events of sponge explants ($n = 6$, $ID\#1-24$), expressed by changes in the relative osculum cross-sectional area (OSA_r).

Treatment	ID #	I (min)	II (min)	III (min)	ΔOSA_{III} (%)	v_I (ΔOSA_r min^{-1})	v_{III} (ΔOSA_r min^{-1})
Untreated	1-6	43 \pm 21	24 \pm 12	74 \pm 39	130 \pm 88	-0.025 \pm 0.010	0.022 \pm 0.020
GABA (1 mM)	7-12	39 \pm 24	22 \pm 9	39 \pm 23	58 \pm 24	-0.032 \pm 0.023	0.015 \pm 0.008
L-Glu (1 mM)	13-18	28 \pm 19	84 \pm 85*	52 \pm 40	68 \pm 54	-0.042 \pm 0.036	0.011 \pm 0.008
Ink particles (4 mg L^{-1})	19-24	59 \pm 41	38 \pm 20	47 \pm 30	150 \pm 114	-0.019 \pm 0.018	0.028 \pm 0.008

I: phase of contraction, II: contracted phase (i.e. $OSA_r = 0$), III: phase of expansion, ΔOSA_I (not shown): relative change in OSA during I, i.e. $-100 \pm 0\%$ across treatments, ΔOSA_{III} : relative change in OSA during III, v_I : contraction rate (determined from the slope of linear regression for changes in ΔOSA_r during I), v_{III} : expansion rate (determined from the slope of linear regression for changes in ΔOSA_r during III). Means \pm SD are shown and significant deviation from spontaneous contraction-expansion events is indicated by * (GLMM, $p < 0.05$).

**FIGURE 3** | *Halichondria panicea*. Spontaneous and induced contraction-expansion dynamics of single-osculum explants, expressed by changes in the relative osculum cross-sectional area and relative projected area (averaged over time \pm 95% confidence intervals). Oscular contraction (I), closure (II) and expansion (III; upper panel) was accompanied by changes in projected area (lower panel), including contraction (I) to a minimum $A_{min} \pm 0.0025$, i.e. the contracted phase (II, horizontal broken lines), expansion (III) and a subsequent expanded phase (IV, vertical broken lines). Slopes of linear regressions (gray lines) indicate mean contraction and expansion speeds for OSA and A . (A) Untreated explants ($ID\#1-6$), (B,C) explants after exposure to the neurotransmitters GABA (1 mM; $ID\#7-12$) and L-Glu (1 mM; $ID\#13-18$), (D) explants after exposure to ink (4 mg L^{-1} ; $ID\#19-24$). Data from **Tables 2, 3**.**TABLE 3** | *Halichondria panicea*. Spontaneous (i.e. untreated conditions) and induced (by exposure to the neurotransmitters GABA, L-Glu or ink particles) contraction-expansion events of sponge explants ($n = 6$, $ID\#1-24$), expressed by changes in the relative projected area (A_r) and relative volume (V_r ; Eq. 3).

Treatment	ID #	I (min)	II (min)	III (min)	ΔA_I (%)	ΔA_{III} (%)	v_I (ΔA_r $\text{min}^{-1} \times 10^{-3}$)	v_{III} (ΔA_r $\text{min}^{-1} \times 10^{-3}$)	ΔV_I (%)	ΔV_{III} (%)
Untreated	1-6	45 \pm 20	7 \pm 2	58 \pm 71	-4.9 \pm 3.0	5.2 \pm 1.8	-1.0 \pm 0.5	2.2 \pm 1.9	-9.6 \pm 5.7	9.5 \pm 3.0
GABA (1 mM)	7-12	47 \pm 29	6 \pm 3	30 \pm 16	-8.1 \pm 5.7	6.8 \pm 8.4	-3.1 \pm 4.0	3.9 \pm 6.7	-15.3 \pm 10.3	11.1 \pm 12.3
L-Glu (1 mM)	13-18	41 \pm 17	12 \pm 6*	106 \pm 77	-11.6 \pm 4.1	5.0 \pm 2.4	-3.5 \pm 3.4*	0.4 \pm 0.2*	-21.6 \pm 7.2*	9.2 \pm 4.1
Ink particles (4 mg L^{-1})	19-24	102 \pm 84	42 \pm 64*	32 \pm 12	-7.3 \pm 4.0	3.0 \pm 2.7	-0.6 \pm 0.3	0.8 \pm 0.7	-13.9 \pm 7.5	5.5 \pm 4.9

I: phase of contraction, II: contracted phase [i.e. $A_r = \min(A_r) \pm 0.025 \text{ mm}^2$], III: phase of expansion, ΔA_I : relative change in A during I, ΔA_{III} : relative change in A during III, v_I : contraction rate (determined from the slope of linear regression for changes in ΔA_r during I), v_{III} : expansion rate (determined from the slope of linear regression for changes in ΔA_r during III), ΔV_I ($=1 - (V_I/V_{max})$): relative volume change during I, ΔV_{III} ($=1 - (V_{III}/V_{max})$): relative volume change during III. Means \pm SD are shown and significant deviation from spontaneous contraction-expansion events is indicated by * (GLMM, $p < 0.05$).

the specimens had an initial (expanded) mean osculum cross-sectional area $OSA_{max} = 0.33 \pm 0.12 \text{ mm}^2$ and a projected area $A_{max} = 30.4 \pm 5.4 \text{ mm}^2$ (Table 5). After

variable exposure time to GABA, the explants were examined in four contractile phases: (I) contracting with closing osculum ($OSA = 0.08 \text{ mm}^2$, i.e. 35% OSA_{max}); (II) contracted with

TABLE 4 | Generalized linear mixed-effect model (GLMM) coefficients (*t*- and *p*-values) for changes in osculum cross-sectional area (OSA) and projected area (*A*) of *Halichondria panicea* explants under different treatments (GABA, L-Glu or Ink) versus untreated conditions (fixed effect), taking into account variability in *A* (fixed effect) and individual variation (*ID#*; random effect).

Treatment	Response variable	GLMM			
		OSA		A	
		<i>t</i>	<i>p</i>	<i>t</i>	<i>p</i>
GABA/untreated	<i>v</i> _I	-0.68	0.496	-2.01	0.161
	<i>v</i> _{III}	1.09	0.278	1.35	0.199
	II	0.29	0.772	0.59	0.553
	ΔV _I	–	–	-1.39	0.164
	ΔV _{III}	–	–	0.48	0.631
L-Glu/untreated	<i>v</i> _I	-0.68	0.190	-2.92	0.015*
	<i>v</i> _{III}	1.84	0.067	2.62	0.020*
	II	-2.55	0.011*	-2.02	0.044*
	ΔV _I	–	–	-2.38	0.018*
	ΔV _{III}	–	–	0.55	0.581
Ink/untreated	<i>v</i> _I	0.83	0.405	0.39	0.695
	<i>v</i> _{III}	-0.80	0.424	-0.03	0.977
	II	-1.20	0.229	-3.53	< 0.001*
	ΔV _I	–	–	-1.20	0.231
	ΔV _{III}	–	–	-0.02	0.980

*v*_I: rate of contraction, *v*_{III}: rate of expansion, II: contracted phase, ΔV _I: relative volume change during contraction (I), ΔV _{III}: relative volume change during expansion (III). Significant deviation from untreated conditions is indicated by * (*p* < 0.05).

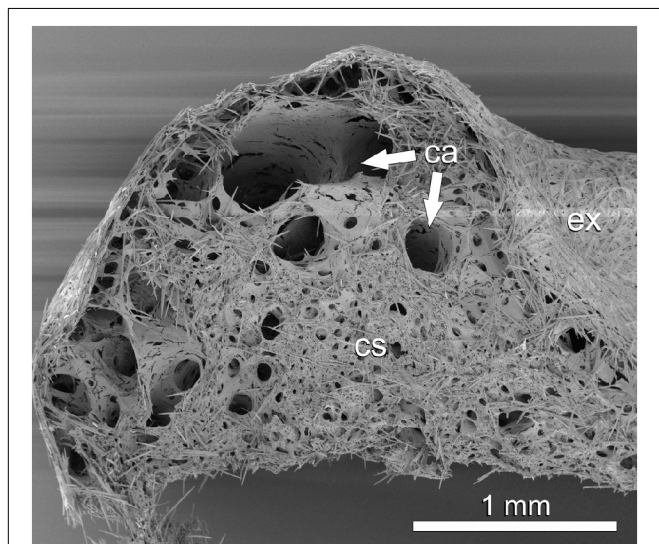


FIGURE 4 | *Halichondria panicea*, SEM, cryofracture. Overview of fracture surface of an expanded explant. Legend: ca: canals, cs: choanosome, ex: exopinacoderm.

completely closed osculum ($OSA = 0.00 \text{ mm}^2$, i.e. 0% OSA_{max}); (III) expanding with re-opening osculum after contraction ($OSA = 0.04 \text{ mm}^2$; i.e. 19% OSA_{max}); and (IV) expanded with open osculum ($OSA = 0.41 \text{ mm}^2$, i.e. 84% OSA_{max} ;

Figure 5A and **Table 5**). Shrinkage due to fixation accounted for $8.4 \pm 4.6\%$ reduction in osculum diameter, indicating a minor impact on our results. The osculum of the contracted explant was completely closed in a sphincter-like fashion with protruding radial bundles of spicules. Similar spicule bundles were not observed around the osculum in the expanded explant (**Figures 5A,B**). The diameter of ostia varied greatly across the four contractile phases I to IV. Compared to the ostia of the expanded explant ($D = 25.0 \pm 3.8 \mu\text{m}$, i.e. 100%; **Figure 5C** and **Table 5**), the diameter of ostia was significantly reduced in the contracting ($D = 14.5 \pm 4.0 \mu\text{m}$, i.e. 58%; GLMM, $t = 7.6$, $p = 4.3 \times 10^{-14}$), contracted ($D = 1.5 \pm 0.5 \mu\text{m}$, i.e. 6%; GLMM, $t = 19.6$, $p < 2 \times 10^{-16}$; **Figure 5D**) and expanding explant ($D = 7.9 \pm 3.9 \mu\text{m}$, i.e. 32%; GLMM, $t = 13.6$, $p < 2 \times 10^{-16}$). The ostia appeared to be associated to porocytes between the exopinacocytes (**Figures 5E,F**). Fractures in the exopinacoderm of the contracted explant (**Figures 5D,F**) were observed, but we interpret these as artifacts caused by sample preparation. Only the expanded and contracted explant could be used for measurements of internal structures due to poor quality of the other cryofractured specimens.

The aquiferous system of the expanded explant had a loosely packed choanosome compared to the contracted explant which appeared more tightly packed (**Figures 6A,B**). Canal diameters varied from $\sim 15 \mu\text{m}$ (directly connected to choanocyte chambers) to $\sim 260 \mu\text{m}$ (large collective in- or excurrent canals) in the expanded explant (**Table 5**) and were significantly reduced to ~ 8 to $\sim 70 \mu\text{m}$ (i.e. to 53% and 27%, respectively), in the contracted explant (**Table 5**; GLMM, $t = 7.7$, $p = 1.2 \times 10^{-14}$). The mean canal diameter after contraction ($D = 24.9 \pm 11.5 \mu\text{m}$) was reduced by 60% compared to the expanded state ($D = 61.7 \pm 48.4 \mu\text{m}$, i.e. 100%), in which canals occupied 32% of the total sponge volume. Apopyle diameters of the contracted explant ($D = 4.7 \pm 1.6 \mu\text{m}$) were reduced by 34% compared to the expanded explant ($D = 7.1 \pm 1.8 \mu\text{m}$, i.e. 100%; GLMM, $t = 8.0$, $p = 1.5 \times 10^{-15}$). In the contracted explant, choanocyte flagella were protruding from the choanocyte chambers into the excurrent canals through the apopylar opening in some cases (**Figure 7A**). Numerous elongated fibers were observed in the subdermal space between the outermost layer of spicules and the choanosome of the contracted explant (**Figure 7B**).

DISCUSSION

Functional Morphology of Contractile Behavior

The present study suggests that GABA-induced contractions of *Halichondria panicea* affect the entire aquiferous system. Similar contraction-expansion dynamics of untreated versus GABA-exposed explants indicate a general sequence of events underlying the contractile behavior of *H. panicea*, and possibly other sponge species. Contraction of *H. panicea* typically involves complete osculum closure for several minutes. Corresponding volume reductions by $\sim 15\%$ after exposure to GABA, as derived from changes in the sponge surface (**Table 3**) reflect observed

TABLE 5 | *Halichondria panicea*. Dimensions of aquiferous elements in single-ostium explants in different contractile phases: I, contracting; II, contracted; III, expanding; IV, expanded; measured after fixation for SEM^a.

Aquiferous element	Morphological state of sponge explants			
	I	II	III	IV
Osculum				
<i>D</i> (μm)	311	51	219	722
OSA (mm ²)	0.08 (<i>N</i> = 1)	0.00 (<i>N</i> = 1)	0.04 (<i>N</i> = 1)	0.41 (<i>N</i> = 1)
Canals				
<i>D</i> (μm)	–	7.6–24.9 ± 11.5–65.7	–	13.8–61.7 ± 48.4*–263.5
<i>A</i> (μm ²)	–	710 ± 665 (<i>N</i> = 37)	–	5006 ± 9172 (<i>N</i> = 51)
Ostia				
<i>D</i> (μm)	7.7–14.5 ± 4.0–26.2	0.6–1.5 ± 0.5–2.7	2.6–7.9 ± 3.9–16.6	17.8–25.0 ± 3.8*–33.5
<i>A</i> (μm ²)	179 ± 107 (<i>N</i> = 50)	2 ± 1 (<i>N</i> = 50)	61 ± 57 (<i>N</i> = 50)	502 ± 152 (<i>N</i> = 50)
Apopyles				
<i>D</i> (μm)	–	1.9–4.7 ± 1.6–8.3	–	3.5–7.1 ± 1.8*–12.4
<i>A</i> (μm ²)	–	21.1 ± 15.2 (<i>N</i> = 51)	–	47.6 ± 20.4 (<i>N</i> = 54)

D: diameter; OSA: osculum cross-sectional area; *A*: projected area; *N*: number of replicate measurements. Minimum – mean (±SD) – maximum values (*D*) or mean values (±SD; *A*) are shown; significant differences between morphological states (I–IV) are indicated by * (GLMM, *p* < 0.05).

changes in internal morphology, as expressed by an estimated volume of (<0.6 × 15%) > 25% comprised by canals relative to the total sponge volume considering a reduction in canal diameters by up to 60% (Table 5). Constriction of the canal system may cause considerable volume changes depending on the morphology of a sponge species. The demosponge *Tethya wilhelma* for instance, which has an extensive bypass- and recirculation-system that connects main excurrent canals with a lacunar system (Nickel et al., 2006), reduces its entire volume by 42–73% during contractions, as expressed by much faster (~10³-fold) contraction and expansion speeds of its projected area (Nickel, 2004) compared to our observations in *H. panicea*. Also, *T. wilhelma* contracts considerably faster than it expands (Nickel, 2004) which was not the case for *H. panicea*. Nevertheless, spontaneous contractions of *T. wilhelma* occur regularly at intervals of 1–10 h (Nickel, 2004) which is comparable to a mean expanded phase 4.2 ± 0.9 h across treatments for the present *H. panicea* explants.

Our study suggests a distinct temporal sequence of coordinated movement during contractions which may be comparable to that described for the freshwater sponge *Ephydatia muelleri* (Elliott and Leys, 2007). Contraction rates seem to be region-specific as a peristaltic-like wave of contraction travels through the different components of the aquiferous system in *H. panicea* (Goldstein et al., 2019); in *E. muelleri* speeds range from 6 to 122 μm s⁻¹ for the osculum, from 0.3 to 4 μm s⁻¹ for peripheral/central canals and from 0.2 to 0.7 μm s⁻¹ for the ostia (Elliott and Leys, 2007). Comparatively, the speed of propagation of the contraction in *H. panicea* explants appears ~1000-fold slower after exposure to GABA for 48 min, as can be estimated from observed temporal changes in diameter between expanded and contracted state, i.e. (–(722–51 μm)/2880 s =)

–233 nm s⁻¹ for the osculum, (–(61.7–24.9 μm)/2880 s =) –13 nm s⁻¹ for the canals, (–(25.0–1.5 μm)/2880 s =) –8 nm s⁻¹ for the ostia and (–(7.1–4.7 μm)/2880 s =) –0.8 nm s⁻¹ for the apopyles (Table 5). The observed dimensions of ostia, canals and osculum of the expanded explant in this study are consistent with a previous study on *H. panicea* (Reiswig, 1975). Based on corresponding changes in the aquiferous system of a contracting explant, we hypothesize contraction-expansion events that initiate with contraction and closure of the osculum (Δ*D* = –100%) and ostia (Δ*D* = –94%), constriction of ex- and incurrent canals (Δ*D* = –60%), contraction of choanocyte chambers (CCs) by means of contractile apopyles (Δ*D* = –34%; Table 5) which may be followed by expansion of the osculum, relaxation of canals, CCs, and opening of ostia. Present observations on the aquiferous elements of cryofractured sponge explants represent a first overview of the morphological changes involved in contraction-expansion events. Follow-up studies may further unravel the temporal dynamics underlying coordinated behavior in sponges.

Observed changes in external and internal sponge volume during GABA-induced contractions may further provide support for pinacoderm-mediated contractions (Nickel et al., 2011) in *H. panicea* which seem to involve constriction of the exopinacoderm around the osculum and pronounced contractions of the endopinacoderm lining the canal system (Goldstein et al., 2019). Accompanying compression of the choanoderm in *H. panicea* is similar to that observed in *T. wilhelma* where especially larger canals and open cavities may disappear completely during contraction due to equally pronounced exo- and endopinacoderm contractions (Nickel et al., 2011). In comparison, the contractility of the exopinacoderm of *H. panicea* seems to be weaker, which is

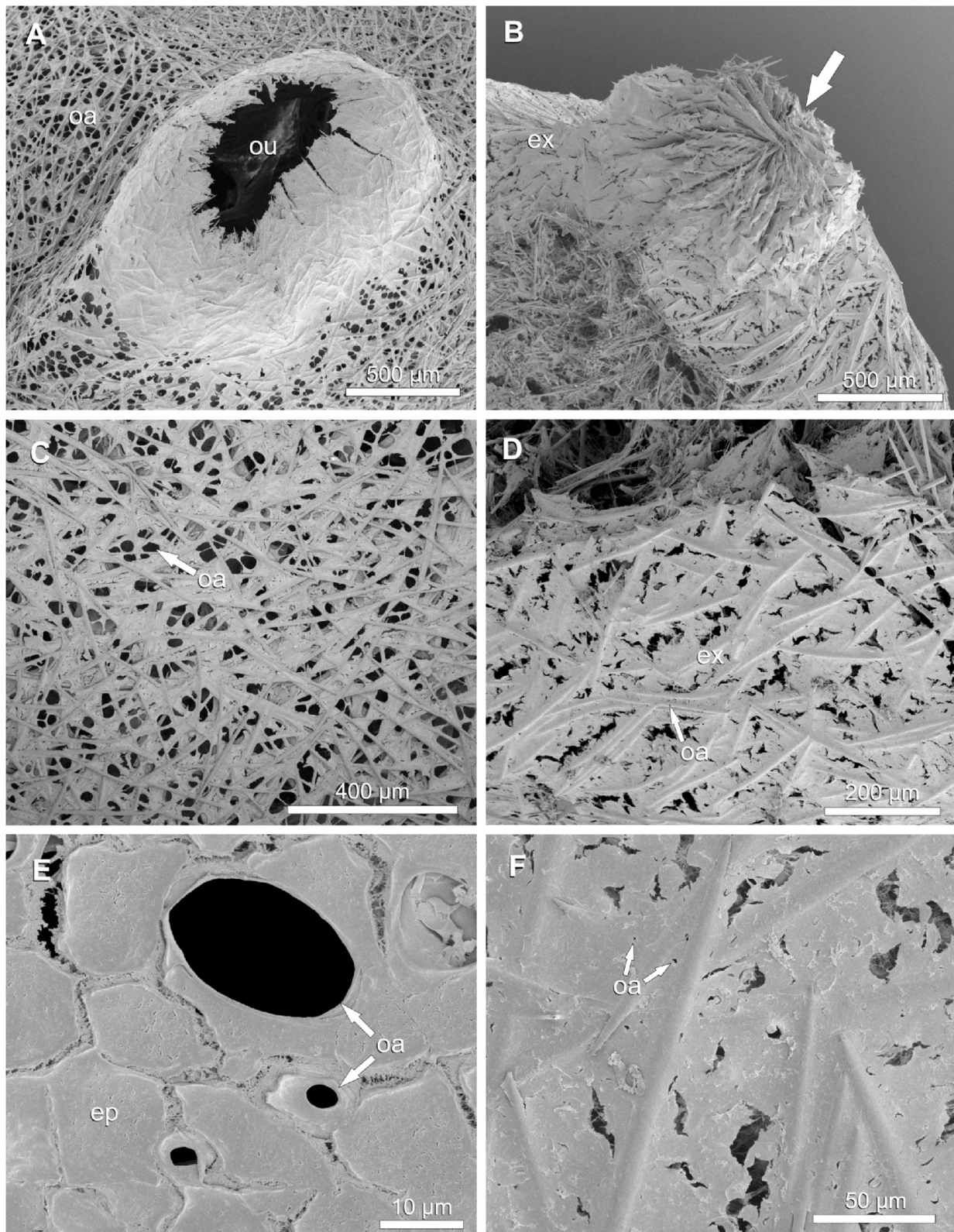


FIGURE 5 | *Halichondria panicea*, SEM. External morphology of expanded and contracted single-ostulum explants. **(A,C,E)** Expanded, untreated explant; **(B,D,F)** contracted explant after exposure to 1 mM GABA. **(A)** Osculum, expanded. **(B)** Closed osculum, note arrangement of radial spicule bundles (arrow). **(C)** Exopinacoderm with high density of expanded ostia. **(D)** Exopinacoderm with closed ostia. **(E)** Three ostia (porocytes) with variable degree of openness. **(F)** Close-up view of ostia during contraction of the sponge explant. Legend: ep: exopinacocyte, ex: exopinacoderm, oa: ostia, ou: osculum.

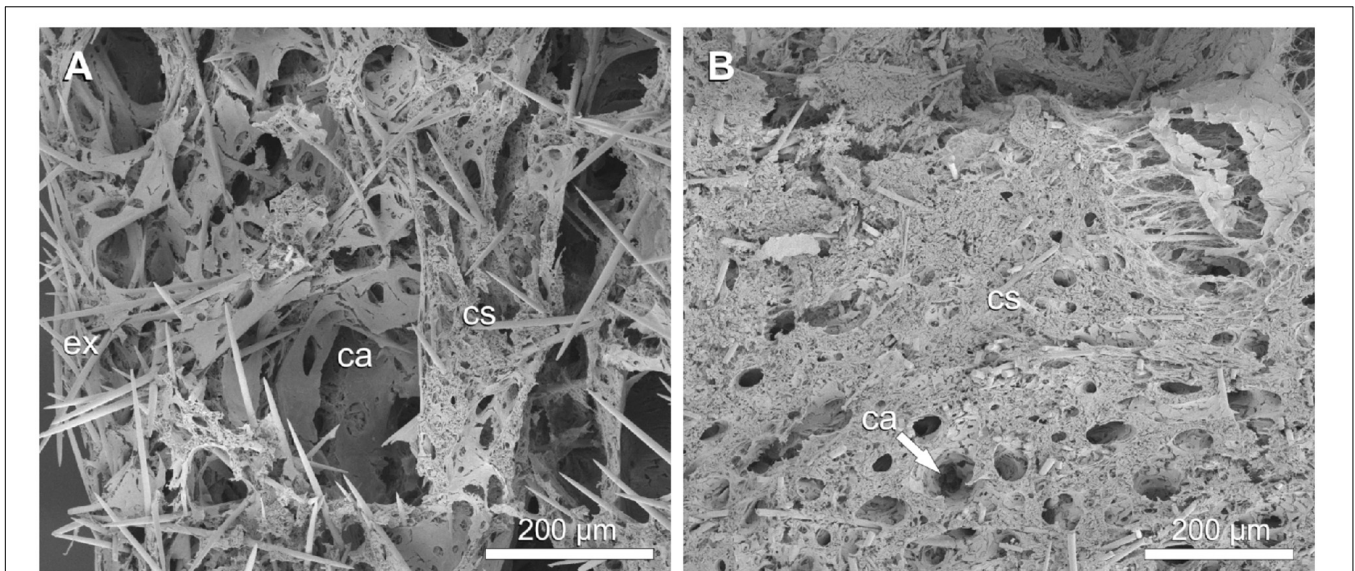


FIGURE 6 | *Halichondria panicea*, SEM, cryofracture. Internal morphology of single-osculum explants. **(A)** Expanded (untreated) explant, choanosome with several larger and smaller canals (ca). **(B)** Contracted explant (after exposure to 1 mM GABA), choanosome mostly with minor canals (ca). Legend: ca: canal, cs: choanosome, ex: exopinacoderm.

indicated by the presence of a spacious cavity characterized by many long fibers stretching between the exopinacoderm and the highly compressed choanosome in the contracted sponge (**Figure 7B**). Radially arranged spicule bundles held together by collagen fibers protruding around the contracted osculum have previously been observed in the demosponge *Haliclona* sp. and could serve as an elastic force to reopen the osculum after contraction (Jones, 1962). Contractile behavior of *H. panicea* is therefore likely driven by an antagonist

system which is based on the interplay between contractile pinacoderm cells, water pressure in the canal system and visco-elastic forces of a collagenous matrix with motile cells in the mesohyl (Elliott and Leys, 2007; Nickel et al., 2011; Hammel and Nickel, 2014). Recent work has further described a novel, yet abundant, choanocyte-related cell type in the mesohyl of a freshwater demosponge (myopeptidocyte) which is likely involved in contraction-expansion of sponges (Musser et al., 2019).

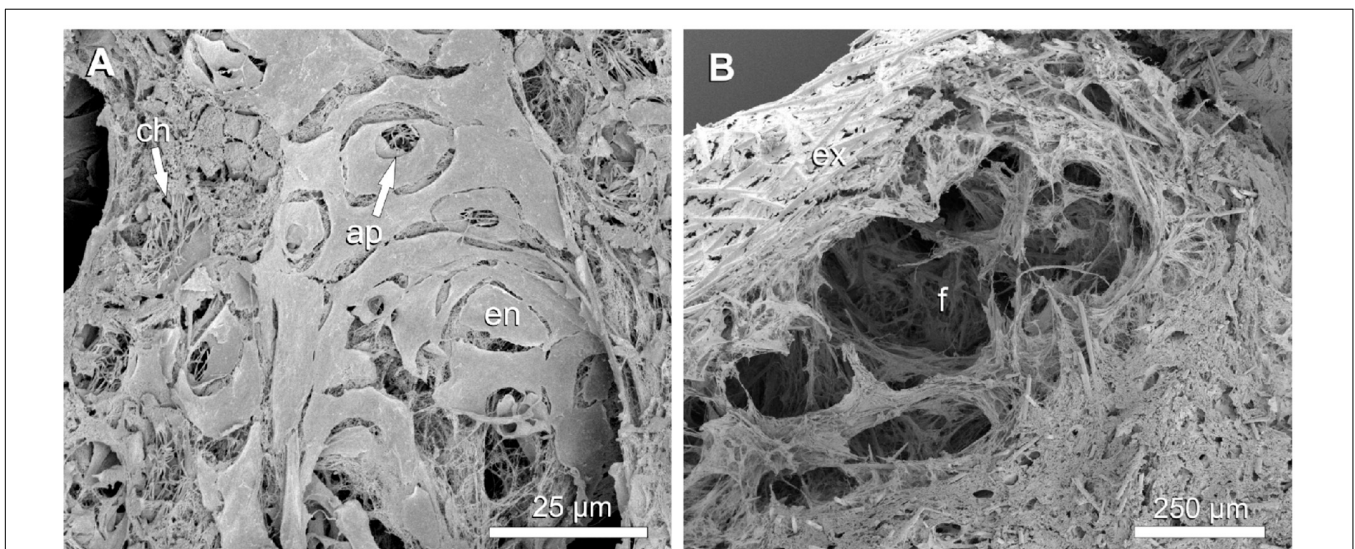


FIGURE 7 | *Halichondria panicea*, SEM, cryofracture. Internal morphology of a contracted (after exposure to 1 mM GABA) single-osculum explant. **(A)** Excurrent canal with constricted apopyles and choanocyte flagella protruding into the canal. **(B)** Cavity with stretched fibers between choanosome and exopinacoderm. Legend: ap: apopyle, ch: choanocyte chamber, en: endopinacocyte, ex: exopinacoderm, f: fibers.

Ecological Role of Contractions in Sponges

Contractions may protect the sponge filter-pump from mechanical damage (Nickel, 2004; Elliott and Leys, 2007) caused by environmental disturbances such as overloading with re-suspended sediment (Reiswig, 1971; Strehlow et al., 2016). In this study, exposure to high concentrations of inedible ink particles significantly prolonged the contracted phase of internal structures (expressed as changes in A and V ; **Table 3**; Nickel, 2004) but not the duration of osculum closure. Also, we observed similar contraction and expansion speeds during ink-induced contractions compared to untreated conditions (**Tables 2, 3**), emphasizing the role of contractile behavior as possible protection mechanism. Compared to *E. muelleri* which has shown an osculum contraction rate of $18 \pm 8 \mu\text{m s}^{-1}$ (entire cycle duration of “ink” fed sponges: 31 min; Elliott and Leys, 2007) after exposure to ~ 6 -fold higher ink concentrations as in the present study (4×10^3 -fold diluted ink; Elliott and Leys, 2007), the speed of propagation of the contraction across the pinacoderm of our *H. panicea* explants was 100-fold slower, i.e. $v_l = -155 \text{ nm s}^{-1}$ [based on $\Delta D (= 2\sqrt{(0.24 \text{ mm}^2/\pi) - 0 \text{ mm}}) = 0.55 \text{ mm}$ within a contraction phase of 59 min; see **Tables 1, 2**]. Along with a prolonged contracted phase of internal structures (**Tables 3, 4**), our observations confirm previous observations that addition of inedible particles slows down contractile behavior (Elliott and Leys, 2007). The particle loads in this study are in the lower range of suspended sediment concentrations occurring in inner-shelf regions of the North Sea (Fettweis et al., 2010; Tjensvoll et al., 2013), emphasizing the ecological relevance of a contractile response mechanism to protect the sponge filter-pump from overloading with inedible particles. Coordinated peristaltic waves have additionally been shown to expel waste material from the aquiferous system of *E. muelleri* (Elliott and Leys, 2010). In *H. panicea*, however, cellular transport mechanisms seem to remove inedible particles from the aquiferous system (Goldstein et al., 2019).

Functional Pathways

The present study supports the presence of a glutamate and GABA receptor signaling system (Perovic et al., 1999) in *H. panicea* and emphasizes that chemical messengers specifically induce contraction (GABA, L-Glu, ink) or expansion (L-menthol) of distinct aquiferous components of a sponge. While the effect of GABA resembled the spontaneous (untreated) contraction-expansion cycle, L-Glu significantly enhanced the rate of contraction and decelerated the rate of expansion of the external sponge surface (**Table 3**). Further, exposure to L-Glu prolonged the duration of osculum closure and subsequent contracted phase of the external surface (**Tables 2, 3**) and led to significantly increased reductions in sponge volume during contraction (**Table 3**). An inhibitory action of GABA and excitatory effect of glutamate has previously been observed in *E. muelleri* (Elliott and Leys, 2010). However, exposure of *H. panicea* explants to GABA did not inhibit contractions as observed in *E. muelleri* (Elliott and Leys,

2010) but triggered contractions at a final concentration of 1 mM, similarly as observed in *T. wilhelma* after exposure to 0.1 mM GABA (Ellwanger et al., 2007). As indicated by a ~ 100 -fold difference in the glutamate concentration to induce full contractions in *E. muelleri* (0.08 mM; Elliott and Leys, 2010) or *T. wilhelma* (10 mM; Ellwanger et al., 2007), respectively, physiological levels and effects of chemical messengers may vary across sponge species (Ellwanger and Nickel, 2006; Ellwanger et al., 2007; Elliott and Leys, 2010). Coordinated contractile responses of demosponges in part also seem to be regulated through nitric-oxide (NO) signaling (Ellwanger and Nickel, 2006; Elliott and Leys, 2010; Musser et al., 2019), which triggers relaxation of endothelial smooth muscle contraction in vertebrates (Palmer et al., 1987). An improved understanding of contractions in sponges on a cellular level may thus provide some fundamental insights into the evolution of nervous systems and muscle tissue in metazoans.

CONCLUSION

The excitatory effect of the neurotransmitter GABA made it possible to study the internal and external morphology of *Halichondria panicea* during induced contraction-expansion events. SEM of sponge explants in different contractile phases suggested gradual changes in the entire aquiferous system, including osculum, ostia, in- and excurrent canals and apopyles. The present findings emphasize the interplay between environmental and/or intrinsic cues, signal transduction via chemical messengers and functional cell morphology for coordinating contractile behavior in sponges.

DATA AVAILABILITY STATEMENT

All datasets generated for this study are included in the article/**Supplementary Material**.

ETHICS STATEMENT

The study was conducted on marine sponges (invertebrates) and therefore was exempted from this requirement.

AUTHOR CONTRIBUTIONS

JG conducted research on the contraction-expansion dynamics of sponge explants, analyzed the data, and wrote the manuscript. NB and PF conducted the morphological study of sponge explants using scanning electron microscopy (SEM) and wrote the manuscript. HR led the experimental design and wrote the manuscript.

FUNDING

This work was supported by a research grant (9278) from the VILLUM FONDEN and a grant (8021-00392B) from the Independent Research Fund Denmark.

REFERENCES

- Asadzadeh, S. S., Larsen, P. S., Riisgård, H. U., and Walther, J. H. (2019). Hydrodynamics of the leucon sponge pump. *J. R. Soc. Interface* 16:20180630. doi: 10.1098/rsif.2018.0630
- Bannister, R. J., Battershill, C. N., and De Nys, R. (2012). Suspended sediment grain size and mineralogy across the continental shelf of the Great Barrier Reef: impacts on the physiology of a coral reef sponge. *Cont. Shelf Res.* 32, 86–95. doi: 10.1016/j.csr.2011.10.018
- Bates, D., Mächler, M., Bolker, B., and Walker, S. (2014). Fitting linear mixed-effects models using lme4. *J. Stat. Softw.* 67, 1–48.
- Elliott, G. R., and Leys, S. P. (2007). Coordinated contractions effectively expel water from the aquiferous system of a freshwater sponge. *J. Exp. Biol.* 210, 3736–3748. doi: 10.1242/jeb.003392
- Elliott, G. R., and Leys, S. P. (2010). Evidence for glutamate, GABA and NO in coordinating behaviour in the sponge, *Ephydatia muelleri* (Demospongiae, Spongillidae). *J. Exp. Biol.* 213, 2310–2321. doi: 10.1242/jeb.039859
- Ellwanger, K., Eich, A., and Nickel, M. (2007). GABA and glutamate specifically induce contractions in the sponge *Tethya wilhelma*. *J. Comp. Physiol. A* 193, 1–11. doi: 10.1007/s00359-006-0165-y
- Ellwanger, K., and Nickel, M. (2006). Neuroactive substances specifically modulate rhythmic body contractions in the nerveless metazoan *Tethya wilhelma* (Demospongiae, Porifera). *Front. Zool.* 3:7. doi: 10.1186/1742-9994-3-7
- Erpenbeck, D., Knowlton, A. L., Talbot, S. L., Highsmith, R. C., and van Soest, R. W. M. (2004). A molecular comparison of Alaskan and North East Atlantic *Halichondria panicea* (Pallas 1766) (Porifera: Demospongiae) populations. *Boll. Mus. Ist. Biol. Univ. Genova* 68, 319–325.
- Fettweis, M., Francken, F., van den Eynde, D., Verwaest, T., Janssens, J., and van Lancker, V. (2010). Storm influence on SPM concentrations in a coastal turbidity maximum area with high anthropogenic impact (southern North Sea). *Cont. Shelf Res.* 30, 1417–1427. doi: 10.1016/j.csr.2010.05.001
- Goldstein, J., Riisgård, H. U., and Larsen, P. S. (2019). Exhalant jet speed of single-osculum explants of the demosponge *Halichondria panicea* and basic properties of the sponge-pump. *J. Exp. Biol. Ecol.* 511, 82–90. doi: 10.1016/j.jembe.2018.11.009
- Grant, N., Matveev, E., Kahn, A. S., Archer, S. K., Dunham, A., Bannister, R. J., et al. (2019). Effect of suspended sediments on the pumping rates of three species of glass sponge in situ. *Mar. Ecol. Prog. Ser.* 615, 79–101.
- Hammel, J. U., and Nickel, M. (2014). A new flow-regulating cell type in the demosponge *Tethya wilhelma* – functional cellular anatomy of a leuconoid canal system. *PLoS One* 9:e113153. doi: 10.1371/journal.pone.0113153
- Hothorn, T., Bretz, F., Westfall, P., Heiberger, R. M., Schützenmeister, A., and Scheibe, S. (2013). *Package 'Multcomp': Simultaneous Inference in General Parametric Models. R Package Version 1.2.13.*
- Jones, W. C. (1962). Is there a nervous system in sponges? *Biol. Rev.* 37, 1–47. doi: 10.1111/j.1469-185x.1962.tb01602.x
- Kealy, R. A., Busk, T., Goldstein, J., Larsen, P. S., and Riisgård, H. U. (2019). Hydrodynamic characteristics of aquiferous modules in the demosponge *Halichondria panicea*. *Mar. Biol. Res.* 51, 531–540. doi: 10.1080/17451000.2019.1694691
- Kumala, L., Riisgård, H. U., and Canfield, D. E. (2017). Osculum dynamics and filtration activity studied in small single-osculum explants of the demosponge *Halichondria panicea*. *Mar. Ecol. Prog. Ser.* 572, 117–128. doi: 10.3354/meps12155
- Larsen, P. S., and Riisgård, H. U. (1994). The sponge pump. *J. Theor. Biol.* 168, 53–63. doi: 10.1006/jtbi.1994.1087
- Leys, S. P. (2015). Elements of a 'nervous system' in sponges. *J. Exp. Biol.* 218, 581–591. doi: 10.1242/jeb.110817
- Ludeman, D. A., Farrar, N., Riesgo, A., Paps, J., and Leys, S. P. (2014). Evolutionary origins of sensation in metazoans: functional evidence for a new sensory organ in sponges. *BMC Evol. Biol.* 14:3. doi: 10.1186/1471-2148-14-3
- Ludeman, D. A., Reidenbach, M. A., and Leys, S. P. (2017). The energetic cost of filtration by demosponges and their behavioural response to ambient currents. *J. Exp. Biol.* 220, 995–1007. doi: 10.1242/jeb.146076
- McNair, G. T. (1923). Motor reactions of the fresh-water sponge, *Ephydatia fluviatilis*. *Biol. Bull.* 44, 153–166. doi: 10.2307/1536773
- Musser, J. M., Schippers, K. J., Nickel, M., Mizzon, G., Kohn, A. B., Pape, C., et al. (2019). Profiling cellular diversity in sponges informs animal cell type and nervous system evolution. *BioRxiv* doi: 10.1101/758276 [Preprint]
- Nickel, M. (2004). Kinetics and rhythm of body contractions in the sponge *Tethya wilhelma* (Porifera: Demospongiae). *J. Exp. Biol.* 207, 4515–4524. doi: 10.1242/jeb.01289
- Nickel, M. (2010). Evolutionary emergence of synaptic nervous systems: what can we learn from the non-synaptic, nerveless Porifera? *Invertebr. Biol.* 129, 1–16. doi: 10.1111/j.1744-7410.2010.00193.x
- Nickel, M., Donath, T., Schweikert, M., and Beckmann, F. (2006). Functional morphology of *Tethya* species (Porifera): 1. Quantitative 3D-analysis of *Tethya wilhelma* by synchrotron radiation based X-ray microtomography. *Zoomorphology* 125, 209–223. doi: 10.1007/s00435-006-0021-1
- Nickel, M., Scheer, C., Hammel, J. U., Herzen, J., and Beckmann, F. (2011). The contractile sponge epithelium sensu lato – body contraction of the demosponge *Tethya wilhelma* is mediated by the pinacoderm. *J. Exp. Biol.* 214, 1692–1698. doi: 10.1242/jeb.049148
- Palmer, R. M. J., Ferrige, A. G., and Moncada, S. (1987). Nitric oxide release accounts for the biological activity of endothelium-derived relaxing factor. *Nature* 327, 524–526. doi: 10.1038/327524a0
- Parker, G. H. (1910). The reactions of sponges, with a consideration of the origin of the nervous system. *J. Exp. Zool.* 8, 1–41. doi: 10.1002/jez.1400080102
- Perovic, S., Krasko, A., Prokic, I., Müller, I. M., and Müller, W. E. (1999). Origin of neuronal-like receptors in Metazoa: cloning of a metabotropic glutamate/GABA-like receptor from the marine sponge *Geodia cydonium*. *Cell Tissue Res.* 296, 395–404. doi: 10.1007/s004410051299
- R Core Team (2015). *R: A Language and Environment for Statistical Computing*. Vienna: R Foundation for Statistical Computing.
- Reiswig, H. M. (1971). In situ pumping activities of tropical Demospongiae. *Mar. Biol.* 9, 38–50. doi: 10.1007/bf00348816
- Reiswig, H. M. (1975). The aquiferous systems of three marine Demospongiae. *J. Morphol.* 145, 493–502. doi: 10.1002/jmor.1051450407
- Riisgård, H. U., Kumala, L., and Charitonidou, K. (2016). Using the F/R-ratio for an evaluation of the ability of the demosponge *Halichondria panicea* to nourish solely on phytoplankton versus free-living bacteria in the sea. *Mar. Biol. Res.* 12, 907–916. doi: 10.1080/17451000.2016.1206941
- Riisgård, H. U., and Larsen, P. S. (2000). Comparative ecophysiology of active zoobenthic filter feeding, essence of current knowledge. *J. Sea Res.* 44, 169–193. doi: 10.1016/s1385-1101(00)00054-x
- Strehlow, B. W., Jørgensen, D., Webster, N. S., Pineda, M. C., and Duckworth, A. (2016). Using a thermistor flowmeter with attached video camera for

SUPPLEMENTARY MATERIAL

The Supplementary Material for this article can be found online at: <https://www.frontiersin.org/articles/10.3389/fmars.2020.00113/full#supplementary-material>

- monitoring sponge excurrent speed and oscular behaviour. *PeerJ* 4:e2761. doi: 10.7717/peerj.2761
- Tjensvoll, I., Kutti, T., Fosså, J. H., and Bannister, R. J. (2013). Rapid respiratory responses of the deep-water sponge *Geodia barretti* exposed to suspended sediments. *Aquat. Biol.* 19, 65–73. doi: 10.3354/ab00522
- Tompkins-MacDonald, G. J., and Leys, S. P. (2008). Glass sponges arrest pumping in response to sediment: implications for the physiology of the hexactinellid conduction system. *Mar. Biol.* 154, 973–984. doi: 10.1007/s00227-008-0987-y

Conflict of Interest: The authors declare that the research was conducted in the absence of any commercial or financial relationships that could be construed as a potential conflict of interest.

Copyright © 2020 Goldstein, Bisbo, Funch and Riisgård. This is an open-access article distributed under the terms of the Creative Commons Attribution License (CC BY). The use, distribution or reproduction in other forums is permitted, provided the original author(s) and the copyright owner(s) are credited and that the original publication in this journal is cited, in accordance with accepted academic practice. No use, distribution or reproduction is permitted which does not comply with these terms.